YALE
PEABODY
MUSEUM

P.O. BOX 208118 | NEW HAVEN CT 06520-8118 USA | PEABODY.YALE. EDU

JOURNAL OF MARINE RESEARCH

The *Journal of Marine Research,* one of the oldest journals in American marine science, published important peer-reviewed original research on a broad array of topics in physical, biological, and chemical oceanography vital to the academic oceanographic community in the long and rich tradition of the Sears Foundation for Marine Research at Yale University.

An archive of all issues from 1937 to 2021 (Volume 1–79) are available through EliScholar, a digital platform for scholarly publishing provided by Yale University Library at https://elischolar.library.yale.edu/.

Requests for permission to clear rights for use of this content should be directed to the authors, their estates, or other representatives. The *Journal of Marine Research* has no contact information beyond the affiliations listed in the published articles. We ask that you provide attribution to the *Journal of Marine Research*.

Yale University provides access to these materials for educational and research purposes only. Copyright or other proprietary rights to content contained in this document may be held by individuals or entities other than, or in addition to, Yale University. You are solely responsible for determining the ownership of the copyright, and for obtaining permission for your intended use. Yale University makes no warranty that your distribution, reproduction, or other use of these materials will not infringe the rights of third parties.

This work is licensed under a Creative Commons Attribution-NonCommercial-ShareAlike 4.0 International License.
https://creativecommons.org/licenses/by-nc-sa/4.0/

Some Model Experiments on Continental Shelf Waves[1]

D. R. Caldwell, D. L. Cutchin

Department of Oceanography
Oregon State University
Corvallis, Oregon 97331

M. S. Longuet-Higgins

Department of Applied Mathematics
and Theoretical Physics
Cambridge University
Silver Street, Cambridge, England

ABSTRACT

This paper describes some model experiments that verify the theoretical form of continental shelf waves. Both the dispersion relationship and the positions of the orbital gyres are confirmed. The existence of a maximum frequency for each mode, with a corresponding zero group velocity, may be of significance for field observations.

1. *Introduction.* The rotation of the Earth, combined with uneven bottom topography, gives rise to a distinct class of wave—the topographic Rossby wave. Such waves are due essentially to changes in potential vorticity when fluid elements are displaced up or down a slope. The waves tend to be propagated in one direction only, with shallower water to the right in the northern hemisphere.

Waves of this kind were emphasized by Reid (1958) when he studied edge-waves over a beach of uniform gradient. Robinson (1964) has suggested that low-frequency waves, in which the frequency, σ, is small compared with the Coriolis parameter, might account for some observations of the nonhydrostatic response of sea level to atmospheric pressure in Australia (Hamon 1962, 1963, 1966). Both Robinson (1964) and Mysak (1967, 1968) considered, for simplicity, waves of length much greater than the width of the continental margin. Buchwald and Adams (1968) have considered a model in which the depth over the shelf varied exponentially, and have, by neglecting the horizontal divergence (hence the vertical displacement of the free surface), obtained an

1. Accepted for publication and submitted to press 10 September 1971.

analytical solution. Some dispersion relationships for other types of off-shore topography have been calculated by Munk, et al. (1970). Some indications of shelf waves in the ocean have also been found by Mooers and Smith (1968) in tide-gauge records on the coast of Oregon and by Cartwright (1969) in the unusually sharp diurnal currents off the west coast of Scotland.

It seemed to us desirable to test the existence of such waves on a laboratory scale. A demonstration of topographic waves in an annulus (Phillips 1965) was carried out by Ibbetson and Phillips (1967). But with continental shelf waves, one of the boundaries is open and the depth profile differs in other respects. In this note we describe some simple experiments to generate continental shelf waves and test their theoretical dispersion relationship. The method is similar to that used in a recent study of double Kelvin waves (Caldwell and Longuet-Higgins, in press). The dispersion relationship for the shelf waves (with horizontal divergence included) is well verified, as are other salient features of the motion. We discuss certain physical consequences of the dispersion relationship and suggest how field observations might be planned so as to detect such waves unambiguously in the ocean.

2. *Theory.* According to the linearized theory of long waves in a shallow homogeneous rotating sea, the equations of motion may be written:

$$\left.\begin{aligned} \frac{\delta u}{\delta t} - fv &= -g\frac{\delta \zeta}{\delta x}, \\ \frac{\delta v}{\delta t} + fu &= -g\frac{\delta \zeta}{\delta y}, \end{aligned}\right\} \tag{2.1}$$

where x, y are horizontal rectangular coordinates, t is the time, u and v are the horizontal velocity components, ζ is the surface displacement, f is the Coriolis parameter, and g is the acceleration of gravity. If h denotes the undisturbed depth, the equation of continuity is:

$$\frac{\delta \zeta}{\delta t} + \frac{\delta}{\delta x}(hu) + \frac{\delta}{\delta y}(hv) = 0. \tag{2.2}$$

We consider the situation shown in Fig. 1, which represents a simple continental margin. The depth h is a function of only the offshore coordinate y. L denotes the total width of the margin, with h_1 the depth at the shoreline and h_2 the depth in the open ocean beyond the slope. We consider waves of angular frequency σ and of wave number m propagating in the x direction.

If the divergence parameter

$$\varepsilon = \frac{f^2}{m^2 g h_2} \tag{2.3}$$

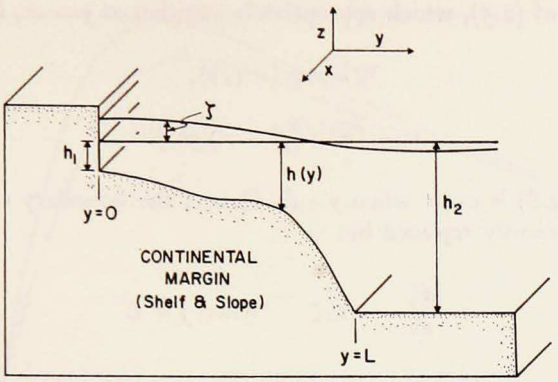

Figure 1. Schematic diagram of a continental margin, showing the axes of x and y. h_1 denotes the depth at the shoreline and h_2 the maximum depth of the ocean. ζ is the surface elevation due to the wave.

is sufficiently small, it may be possible to express the velocity as the curl of a stream-function, as was done by Buchwald and Adams (1968). Though this approximation may be justified in some situations, it is less justifiable in our laboratory model. So we shall retain the full system of eqs. (2.1) and (2.2).

On replacing $\partial/\partial t$ by $-i\sigma$ and $\partial/\partial x$ by im, we may solve (2.1) for the velocity components (u, v):

$$\left.\begin{aligned} u &= \frac{g}{\sigma^2 - f^2}\left(\sigma m\zeta + f\frac{d\zeta}{dy}\right), \\ iv &= \frac{g}{\sigma^2 - f^2}\left(\sigma\frac{d\zeta}{dy} + fm\zeta\right), \end{aligned}\right\} \tag{2.4}$$

and then, on substituting in (2.2), we obtain the differential equation for ζ:

$$\frac{d}{dy}\left(h\frac{d\zeta}{dy}\right) = \left(\frac{f^2 - \sigma^2}{g} + m^2 h - \frac{mf}{\sigma}\frac{dh}{dy}\right)\zeta. \tag{2.5}$$

This equation has been discussed by Longuet-Higgins (1968), who considered solutions over the infinite range $(-\infty < y < \infty)$. Here, however, we have the boundary condition that $hu = 0$ at the shoreline $(y = 0)$. By (2.4) this implies that

$$\frac{d\zeta}{dy} = -\frac{fm}{\sigma}y \quad \text{when } y = 0. \tag{2.6}$$

Further, we have, for a trapped wave,

$$\zeta \to 0 \quad \text{as } y \to \infty. \tag{2.7}$$

The solution of (2.5), which appropriately vanishes as $y \to \infty$, is:

$$\zeta \sim \exp(-\mathrm{I}_2 y), \tag{2.8}$$

where

$$\mathrm{I}_2 = [m^2 + (f^2 - \sigma^2)/gh_2]^{1/2} \tag{2.9}$$

In fact, eq. (2.8) is exact when $y \geq L$. Hence, the boundary condition (2.7) may be conveniently replaced by:

$$\frac{d\zeta}{dy} = -\mathrm{I}_2 \zeta \qquad \text{when } y = L \tag{2.10}$$

and the eigenvalue problem is then solved over the finite interval $0 < y < L$.

To proceed further we must choose a particular profile for the depth, $h(y)$. Then for any given value of the longshore wavenumber, m, the differential equation (2.5), with the boundary conditions (2.6) and (2.10), may be solved numerically by a standard method (see Appendix); this gives a discrete set of eigenfrequencies $\sigma_1, \sigma_2, \ldots\ldots$ and a corresponding set of eigenfunctions $\zeta_1(y), \zeta_2(y), \ldots\ldots$

If the depth profile, $h(y)$, is monotonic, then typically the dispersion relationship (giving the frequency, σ, as a function of the wavenumber) is as shown by the full curves in Fig. 2. All of the eigenfrequencies σ_i are positive, corresponding to waves whose phases progress with the shallower water on their right, in the northern hemisphere. The lowest mode (having the highest frequency) is a Kelvin wave whose velocity, given by the ratio σ/m, tends to

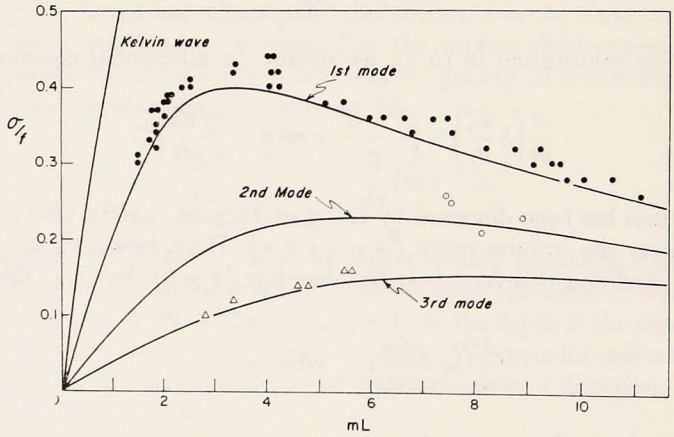

Figure 2. Theoretical curves showing the dependence of the frequency on the longshore wavenumber $m = 2\pi/\text{wavelength}$. The curves are calculated for the profile in Fig. 4. Plotted points represent experimental data.

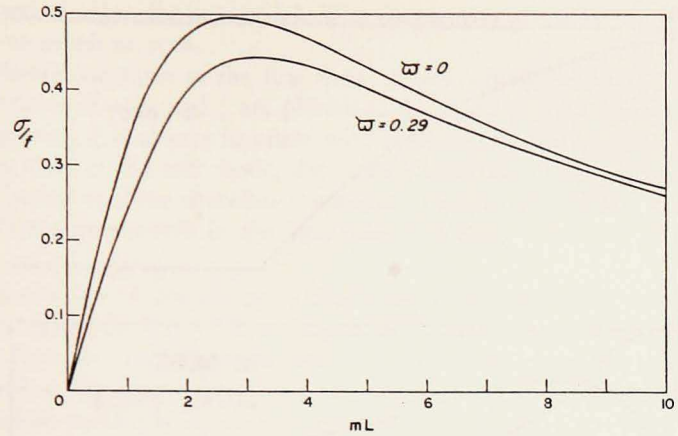

Figure 3. Theoretical dispersion relationship showing the effect of horizontal divergence, in a shelf with exponential profile. The divergence parameter, $\tilde{\omega}$, is defined by eq. (2.11).

the value $(gh_2)^{1/2}$ as $mL \to 0$ (large wavelengths) and tends to $(gh_1)^{1/2}$ as $mL \to \infty$ (small wavelengths). The frequency increases with the wave number, so that the group velocity, $d\sigma/dm$, has the same sign as the phase velocity, σ/m. We shall call this the zeroth mode. The other modes behave differently. Each of their frequencies rises to a maximum at some positive value of mL and tends to zero as $mL \to \infty$, provided of course that $h_1 > 0$. (If a beach condition exists, then σ/f tends to a positive limit). On the low wavenumber side of the maximum the group velocity is positive, and on the high wave number side it is negative. Thus, for any given value of the frequency σ/f that is less than the maximum for a given mode, there are two possible waves: one with positive group velocity and one with negative group velocity. At the maximum frequency, the group velocity vanishes. These waves have special properties, as we shall see below.

If the horizontal divergence were neglected, as in the theory of Buchwald and Adams (1968), the Kelvin wave would not appear; it would tend to coincidence with the σ-axis.

The effect of horizontal divergence on the other modes may be seen in Fig. 3, where the dispersion relationship for the first mode is shown for an exponential profile, $h(y)$, similar to that in our model. The divergence parameter, $\tilde{\omega}$, is defined by

$$\tilde{\omega} = \frac{Lf^2}{gh'}, \tag{2.11}$$

where h' denotes the maximum bottom slope. The curve $\tilde{\omega} = 0$ corresponds to the nondivergent theory of Buchwald and Adams (1968), checked by our numerical integration. The other curve is calculated numerically with $\tilde{\omega} =$

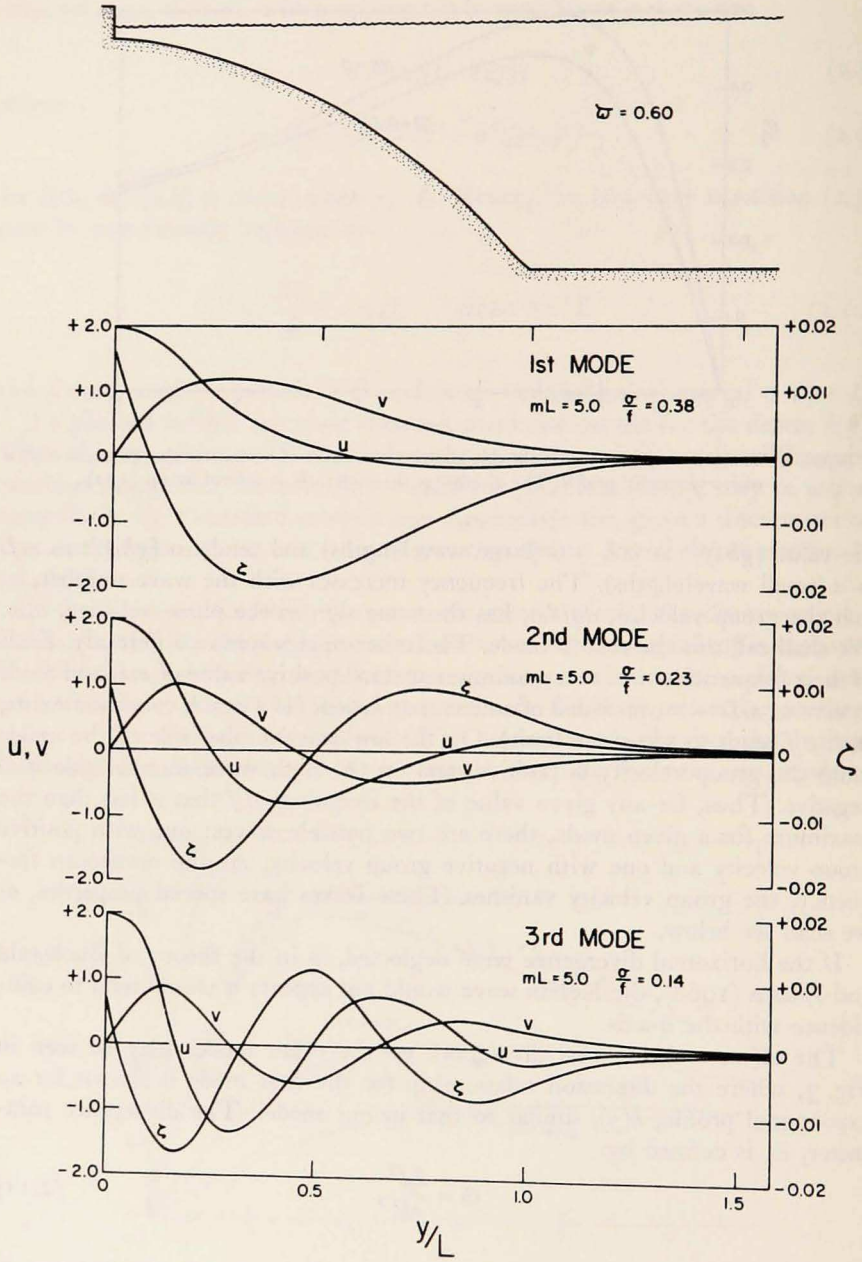

Figure 4. (Top): A cross-section of the wide shelf. (Bottom): The amplitudes of u, v, and ζ in the first three modes, in the typical case $mL = 5.0$. The Kelvin wave is not shown.

0.29, a typical value for our model. The frequencies given by the two curves differ by as much as 20%.

The theoretical form of the first three modes is indicated in Fig. 4, where the amplitudes of u, v, and ζ are plotted as functions of y for typical values of the parameters. ζ is always in phase with u but in quadrature with v. It can be shown that, in the nth mode, the surface elevation ζ has just n zeros. So also have u and v, if the shoreline is counted as a zero of v. Thus, the circulation is divided into n cells in the transverse direction.

3. *Experiments.* A circular model basin was constructed with the axial cross section as shown in Fig. 5. The deep-water section beyond the shelf was of parabolic form, so that when the basin was rotated at a constant speed, $\Omega/2\pi = 0.5$ revs/sec, the depth of water beyond the shelf was uniform when measured in a direction parallel to the axis of rotation.

The total shelf width, L, was 16.0 cm, the depths, h_1 and h_2, were 0.6 cm and 10.0 cm, respectively (measured parallel to the axis). A variation in the shelf was made by moving the simulated shoreline out through a distance $L/2$. The original shelf will be called the "wide shelf", the variation, the "narrow shelf".

The motion was generated by a paddle that oscillated radially, forcing water across the depth contours. The paddle was driven by a d.c. motor whose speed could be varied; the model rotated with a constant period of 2.0 secs (counterclockwise). The paddle period was determined by measuring, with an electronic counter, the time between successive closures of a microswitch tripped by a

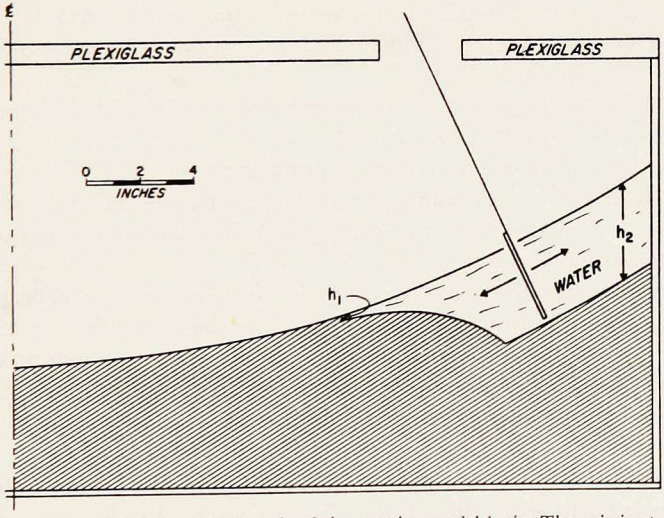

Figure 5. A cross section through the axis of the rotating model basin. The axis is at the left-hand edge.

cam on the motor shaft. The rotation period of the model was measured similarly. The width of the paddle was varied according to the wavelength of the expected motion; it was usually between 1/4 and 1/8 of a wavelength.

We found that the waves were best observed by streak photographs. Aluminum powder was distributed over the water surface and sequences of 16-mm photographs were taken with exposures varying from 0.5 sec to 5 sec (depending on the wave period) and a delay of a few tenths of a second between exposures. The wavelengths were measured directly from the projected frames at the radius of the wave "centers" (see below); the phase speeds were measured by noting the motion of the waves between successive frames. From the phase speed and frequency, independent estimates of the wavelength were computed. In cases where the wavelength was too long for an entire wave to be seen in one picture, these were the only estimates.

Some photographs are shown in Figs. 6 to 8. Fig. 6 shows short waves propagating to the left of the paddle, which is located just to the right of the photograph. Fig. 7 shows long waves on the other side of the paddle, which can be seen at the left of this picture.

In order to generate higher modes, two parallel paddles were used; these moved like scissor blades. The resulting motion of the water is shown in Fig. 8. Measurements of the wave forms (described below) show this to be the third mode.

In Fig. 2 are shown the experimentally determined values of the dimensionless wavenumber, mL, plotted against the ratio of the angular frequency of the wave to the Coriolis parameter, σ/f. We have taken $f = 2\Omega$. All of the data in Fig. 3 correspond to the "wide" shelf. The first and third modes (dots and triangles) could be definitely identified as such from the photographs. The data represented by the open circles, which could not be definitely identified, appear to be second-mode waves.

Fig. 9 compares the first mode frequencies for the wide shelf (upper curve) and for the narrow shelf (lower curve).

The accuracy of the measurements is probably represented fairly well by the scatter of the experimental points. An individual measurement of wavelength could be made with an accuracy of perhaps 2%, but measurements varied from frame to frame by 5–10%.

We also measured the distances from the shoreline to the "centers" of the waves—that is, to the points that appeared to be motionless in the streak photographs—and we compared them with the distances indicated by the eigenfunctions, such as those shown in Fig. 4. The results are given in Table I, where a good measure of agreement is shown.

4. *Discussion.* Figs. 2 and 9 show that the agreement between theory and experiment is fairly good, though the observations tend to be somewhat above the theoretical curves. Some of the possible sources of error are similar to those

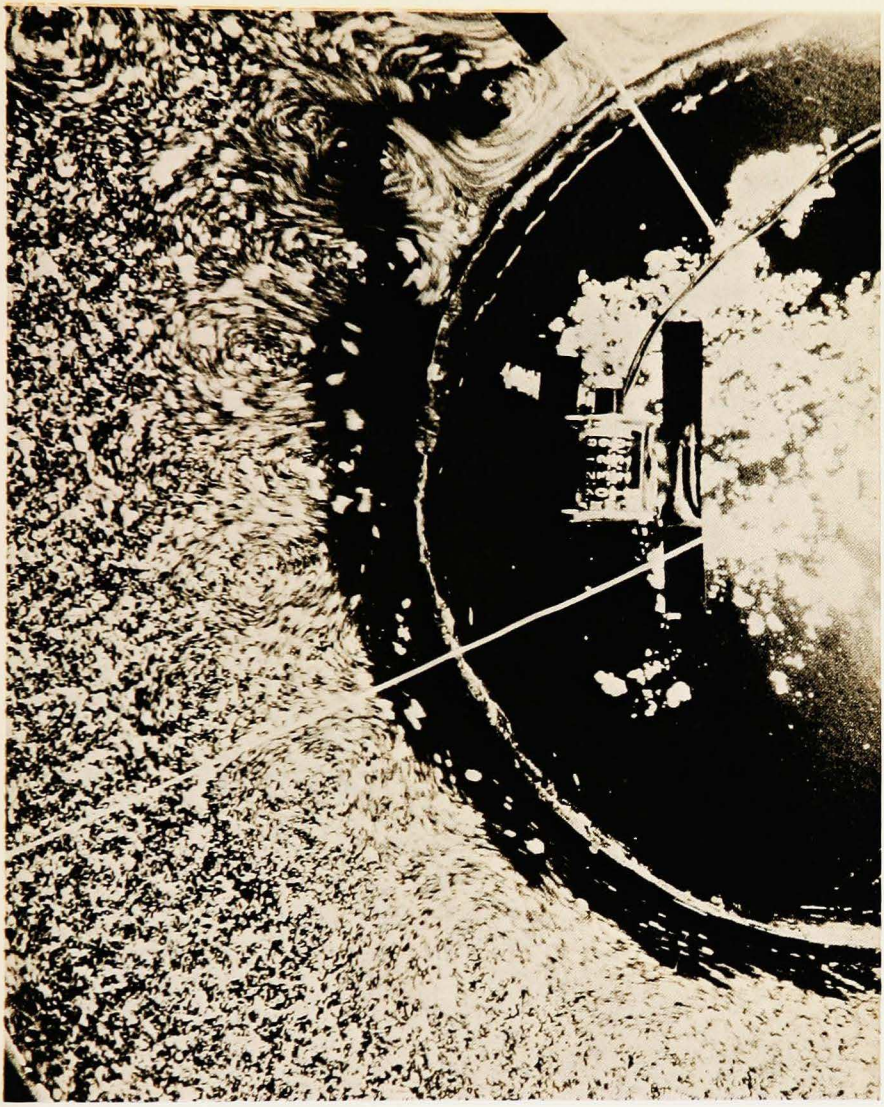

Figure 6. A streak photograph showing short waves propagating "eastward" at a frequency $\sigma/f = 0.30$. The paddle, 4 cm wide and with a 7 cm stroke, is at the top of the picture. The outer edge of the basin is at the left. Exposure: 0.6 sec; paddle period: 3.33 sec.

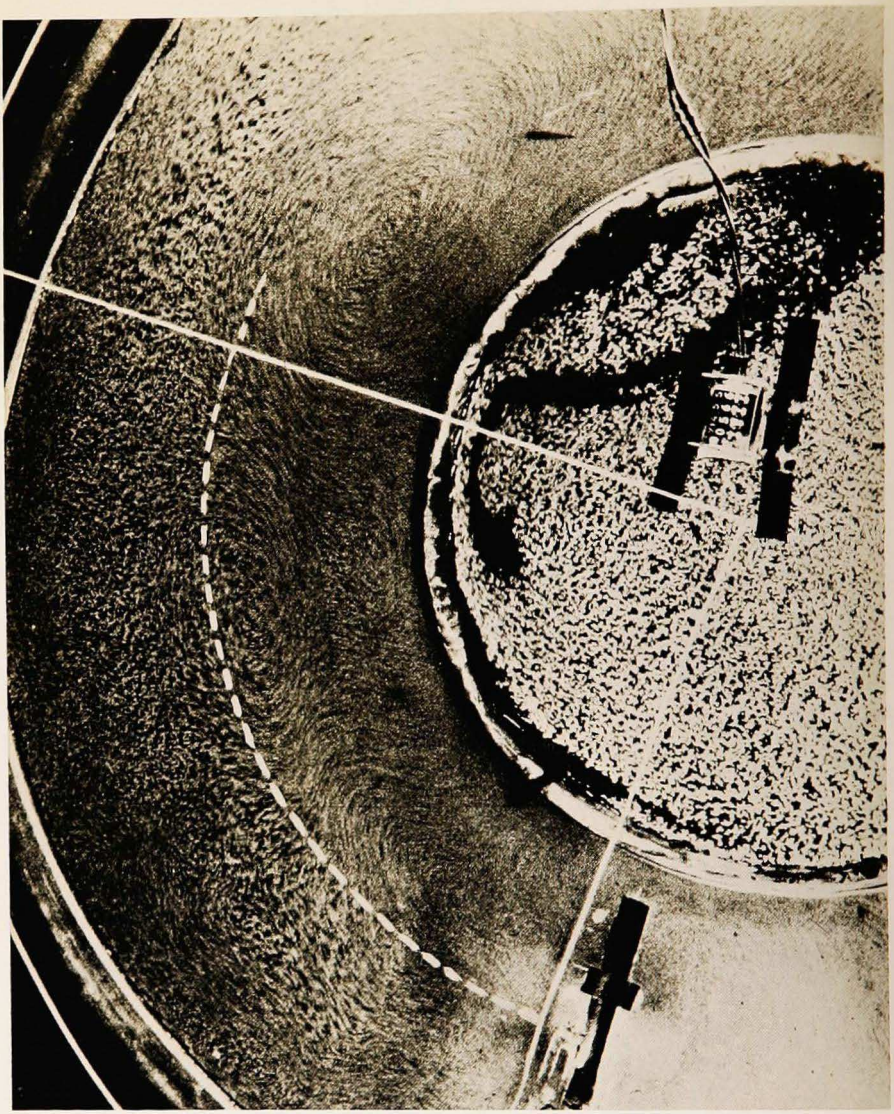

Figure 7. Long waves propagating "westward" at $\sigma/f = 0.37$. The paddle (10 cm wide) is at the bottom Exposure: 0.7 sec; paddle period 2.70 sec. The solid lines are radii. The broken line marks the foot of the slope.

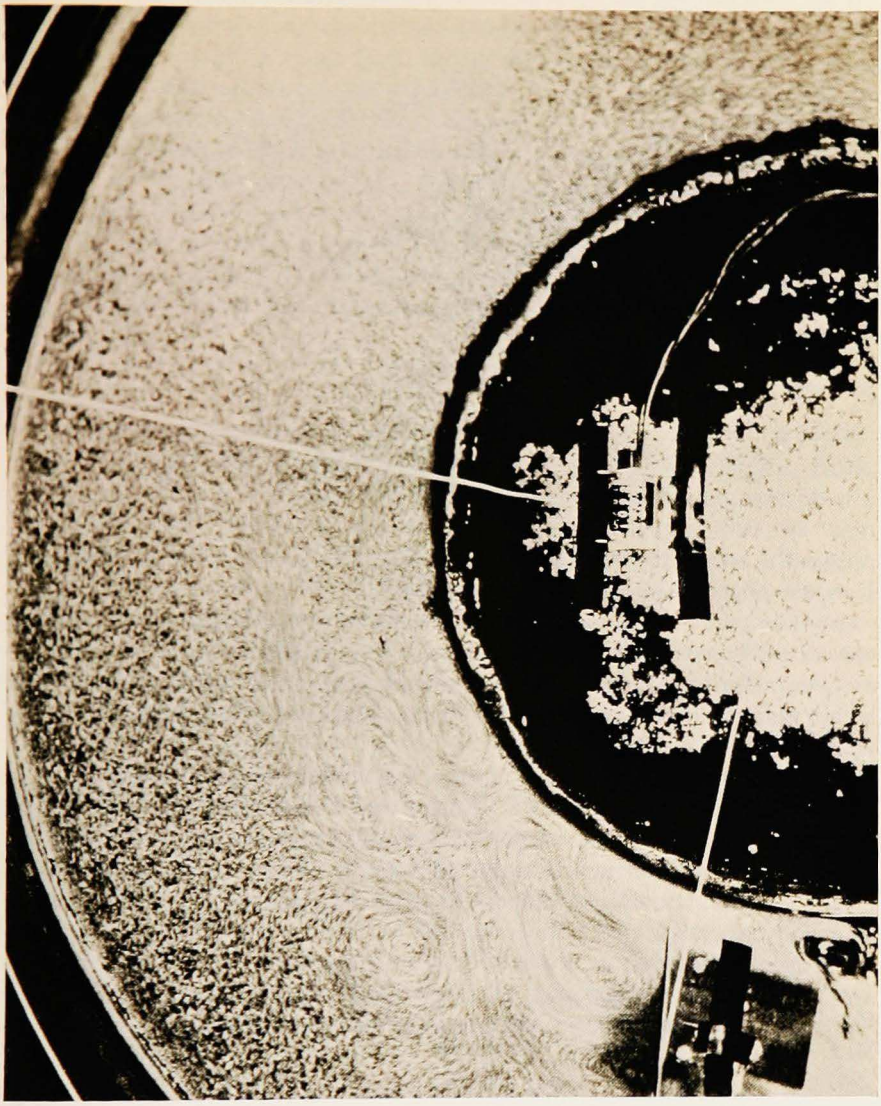

Figure 8. Higher modes generated by a double paddle (10 cm wide, scissors action) which is visible at the bottom. Exposure 0.9 sec; period 7.1 sec.

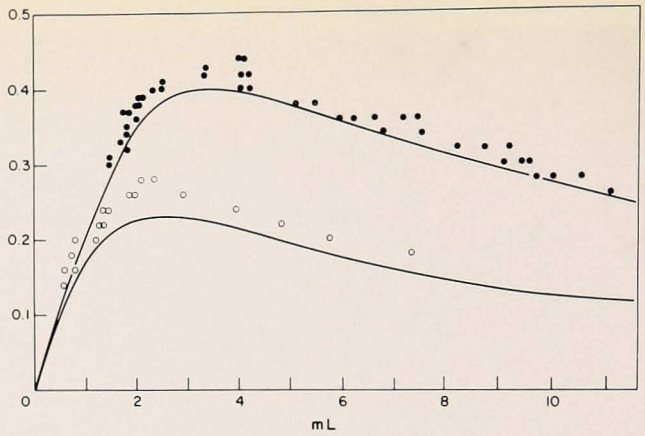

Figure 9. Dispersion curves, relating frequency σ and longshore wave number m, for shelves of two different widths. The upper curve corresponds to the "wide shelf" (L = 16.0 cm) and the lower curve to the "narrow shelf" (L = 8.0 cm). The plotted points represent experimental data.

previously considered in a study of double Kelvin waves by Caldwell and Longuet-Higgins (in press).

(i) The curvature of the contours in a plane perpendicular to the axis was considered by solving the appropriate equation, similar to (2.6), in radial coordinates. For a given wavenumber, the frequency was found to be reduced by not more than 3%, and this effect was confined to the longer waves (smaller wavenumbers).

(ii) The effect of the outer boundary was considered by replacing eq. (2.7) with the condition that the radial velocity vanish at the boundary. This again reduced the theoretical frequency by an amount of the same order of magnitude.

(iii) The effect of the curvature of the free surface in an axial plane is harder to assess, but it is probably of the same order as (1-cos θ), where θ is the

Table I.

Mode	Experimental			Theoretical		
	mL	σ/f	Distance to gyre center*	Distance to node in wave function*	mL	σ/f
1	1.2	0.30	0.81	0.78	1.6	0.30
1	1.5	0.36	0.69	0.75	2.1	0.36
1	2.0	0.41	0.85	0.68	3.0	0.4
1	6.5	0.36	0.72	0.54	5.7	0.37
1	3.5	0.42	0.75	0.68	3.0	0.4
3	2.8	0.14	0.18 0.60 0.97	0.18 0.51 0.91	4.0	0.13

* Distances are scaled by shelf width.

angle between the axis of rotation and the normal to the free surface near the center of the shelf (where the energy density of the motion is greatest). In these experiments, θ is about 30%, so we would expect discrepancies of the order of 15% between theory and experiment. That these discrepancies are not seen suggests that some of the errors mutually cancel.

(iv) The effect of viscosity is mainly felt in boundary layers of thickness $\delta \doteq (2\nu/f)^{1/2}$ on the sides and bottom. Typically, δ is of the order of 0.05 cm. Since this is small compared with the mean depth, $\bar{h}$ (of the order of 1% or less), the main effect on the motion is to introduce damping due to viscous dissipation of energy in the boundary layers. Caldwell and Longuet-Higgins (in press) have shown that the e-folding distance for the wave amplitude is of the order of

$$N = \frac{1}{\pi} \frac{\sigma}{f} \frac{c_g}{c} \frac{\bar{h}}{\delta} \quad \text{wavelengths,}$$

where c and c_g denote the phase velocity, σ/k, and the group velocity, $d\sigma/dk$, respectively. This is comparable to the rate of decay seen in the experiments.

In spite of the possible errors listed above, it may be said that the main features of continental shelf waves have been well verified in the laboratory. In particular there is a clear indication of a maximum frequency, for each mode, implying a vanishing group velocity. Waves of this frequency and wavenumber should tend to "gang around" their point of origin, since their energy is propagated with zero velocity. Hence, oscillations of this frequency should be characteristic of the bottom topography of each particular coastline.

5. *Oceanic Observations of Shelf Waves.* Present indications of shelf waves in the ocean (Hamon 1962, 1963, 1966, Mooers and Smith 1968, Cartwright 1969, Cutchin 1972) are both scanty and indirect. In view of the possibly common occurrence of these waves, it is worthwhile to discuss how best to plan a field investigation designed especially to detect them.

Shelf waves seem most likely to become evident in current records, and, to a lesser extent, in records of surface elevation or bottom pressure. To eliminate baroclinic motions, it is generally necessary to measure current velocities at several different depths in any one vertical line and to take the mean current.

Suppose first that we have records of u, v, and ζ at a single location. We denote these functions of the time by $F_1(t)$, $F_2(t)$, and $F_3(t)$. From such records we may compute the three frequency spectra $E_i(\sigma)$ $(i = 1,2,3)$ and the cospectra and quadrature spectra $C_{ij}(\sigma)$ and $Q_{ij}(\sigma)$, where $C_{ii} \equiv E_i$. Hence, at each frequency, σ, we can calculate the relative phase and amplitude of u, v, and ζ as well as the mutual coherency.

If there is only one mode at a particular frequency, then the coherency will be high, and the coherent parts of u and ζ will be in phase ($Q_{13} \ll C_{13}$); the

coherent parts of v and ζ will be in quadrature ($Q_{23} \ll C_{23}$). Moreover, the relative amplitudes of all the C_{ij} and Q_{ij} will be predictable. In this very simple circumstance we should have a strong indication of a single shelf wave.

But from the dispersion relationship (Fig. 3, for example) we know that there may be two waves of Mode 1, two of Mode 2, and so on, up to a finite number. If this were the case, we would still have $Q_{13} \ll C_{13}$, and $Q_{23} \gg C_{23}$, but the relative amplitudes of the other C_{ij} would not be the same as in any one of the modes.

In some cases we may make a slightly stronger statement. Suppose for instance that there are two waves present, with theoretical cospectra $(C'_{ij} + iQ'_{ij})$ and $(C''_{ij} + iQ''_{ij})$. Then the cospectrum of the combined signal will be of the form:

$$(C_{ij} + iQ_{ij}) = \lambda(C'_{ij} + iQ'_{ij}) + \mu(C''_{ij} + iQ''_{ij}),$$

where λ and μ are constants independent of i, j. Geometrically, if we take $\underset{\sim}{C} \equiv (C_{11}, C_{22}, C_{33}, C_{23}, Q_{12}, Q_{23})$ as homogeneous coordinates in a five-dimensional space, then $\underset{\sim}{C}$ lies on the straight line joining $\underset{\sim}{C}'$ and $\underset{\sim}{C}''$. Similarly, if three modes were present, $\underset{\sim}{C}$ would lie in the plane determined by $\underset{\sim}{C}'$, $\underset{\sim}{C}''$, and $\underset{\sim}{C}'''$; and so on. Such a method is capable, in theory, of determining the relative amplitudes of five independent modes at a given frequency, provided these are the only motions present, from records taken at a single station. But the presence of noise will, in practice, probably confine the usefulness of the method to the case when one or two modes are dominant.

In practice it is very desirable to have more than one current-meter station. A particularly strong confirmation would be obtained from data taken at two or more stations in a line at right angles to the bottom contours. The relative amplitudes of the modes at the different stations should, of course, be the same. A plot of the observed amplitude of each mode as a function of distance offshore could be compared directly with the theory.

To verify the dispersion relationship in detail, it is necessary to have measurements at different stations in a line *parallel* to the coast. If one mode is dominant, then the phase velocity can be determined from the relative phase at any two stations. More ambitiously, we might hope to determine the (σ,m) spectrum, as was done by Munk, et al. (1964) for edge-waves (of much higher frequency) off the coast of California.

A distinguishing feature of the particular low-frequency waves under discussion is the maximum frequency for each mode. In the neighborhood of such a maximum, there is a large spread of wavenumber corresponding to only a very small change in frequency. This makes it more difficult to determine the wavenumber of any particular mode, but there is a compensating advantage: if the spectrum of wavenumbers is continous, as it may be on a uniform straight coastline, then the frequency spectrum $E_i(\sigma)$ at any given station should show

a peak at the maximum modal frequencies. Indeed, one of the first and simplest tests for the presence of shelf waves is whether the theoretical maximum frequencies appear as maxima in the frequency spectra.

Acknowledgments. This work was performed under National Science Foundation grant GA1452 with assistance from the Royal Society of London.

REFERENCES

Buchwald, V. T., and J. K. Adams
1968. The propagation of continental shelf waves. Proc.roy.Soc. London, *A305*: 235–250.

Caldwell, D. R., and M. S. Longuet-Higgins
In press. An experimental investigation of double Kelvin waves. Proc.roy.Soc. London, *A*.

Cartwright, D. E.
1969. Extraordinary tidal currents near St. Kilda. Nature, London, *223*: 928–932.

Cutchin, D. L.
1972. Low frequency variations in the sea level and currents over the Oregon continental shelf. Ph. D. Thesis, Department of Oceanography, Oregon State University, Corvallis, Oregon. 122 pp.

Hamon, B. V.
1962. The spectra of mean sea level at Sydney, Coff's Harbour, and Lord Howe Island. J. geophys. Res., *67*: 5147–5155.
1963. Correction. J. geophys. Res., *68*: 4635.
1966. Continental shelf waves and the effects of atmospheric pressure and wind stress on sea level. J. geophys. Res., *71*: 2883–2893.

Ibbetson, A., and N. A. Phillips
1967. Some laboratory experiments on Rossby waves in a rotating annulus. Tellus, *19*: 81–87.

Longuet-Higgins, M. S.
1968. Double Kelvin waves with continuous depth profiles. J. fluid Mech., *34*: 49–80.

Mooers, C. N. K., and R. L. Smith
1968. Continental shelf waves off Oregon. J. geophys. Res., *73*: 549–557.

Munk, W. H., F. E. Snodgrass, and M. Wimbush
1970. Tides off-shore; transition from California coastal to deep-sea waters. Geophys. fluid Dynam., *1*: 161–235.

Munk, W. H., F. E. Snodgrass, and F. J. Gilbert
1964. Longwaves on the continental shelf; an experiment to separate trapped and leaky modes. J. fluid Mech., *20*: 529–554.

Mysak, L. A.
1967. On the theory of continental shelf waves. J. mar. Res., *25*: 205–227.
1968. Edgewaves on a gently sloping continental shelf of finite width. J. mar. Res., *26*: 24–33.

Phillips, N. A.
1965. Elementary Rossby waves. Tellus, *17*: 295–301.

REID, R. O.
1958. Effect of Coriolis force on edge waves. (1) Investigation of the normal modes. J. mar. Res., *16*: 109–144.

ROBINSON, A. R.
1964. Continental shelf waves and the response of sea level to weather systems. J. geophys. Res., *69*: 367–368.

APPENDIX

To prepare eq. (2.5) for solution over the interval $0 < y < L$, we set

$$\zeta = P(y), \qquad h\frac{d\zeta}{dy} = Q(y) \tag{A1}$$

in the left half of the interval ($0 < y < L/2$) and

$$\zeta = R(y), \qquad \frac{1}{h}\frac{d\zeta}{dy} = S(y) \tag{A2}$$

in the right half ($L/2 < y < L$). Then, in the left half, P and Q satisfy the two linear equations:

$$\left.\begin{aligned} \frac{dP}{dy} &= Q \\ \frac{dQ}{dy} &= \left(\frac{f^2-\sigma^2}{g} + m^2 h - \frac{fm}{\sigma}\frac{dh}{dy}\right) P \end{aligned}\right\} \tag{A3}$$

with similar equations for R, S in the right half. Choosing some value of σ, we now integrate P and Q step-by-step from the left, starting with the initial conditions

$$P = A, \qquad Q = -\frac{fmh}{\sigma}\cdot A \qquad \text{when } y = 0, \tag{A4}$$

where A is some convenient constant (say unity). This makes $v = 0$ when $y = 0$. At the same time, we integrate R and S from the right, starting with the values

$$R = B, \qquad S = -(l_2/h_2)\,B \qquad \text{when } y = L, \tag{A5}$$

where l_2 is given by (2.9). In each case the integration is carried as far as the midpoint $y = L/2$. If P_1, Q_1, R_1, S_1 denote the values of P, Q, R, S, at the midpoint, we now calculate the Wronskian

$$W \equiv P_1 S_1 - Q_1 R_1, \tag{A6}$$

which is a function of the initial frequency σ. If σ were an eigenvalue, then, since both ζ and $d\zeta/dy$ must be continuous at $y = L/2$, the ratios P_1/Q_1 and R_1/S_1 would be equal, making W vanish. Conversely, when W vanishes we can find A and B so that ζ satisfies all the necessary conditions and so that ζ and $d\zeta/dy$ are continuous at $y = L/2$. Hence, the eigenfrequencies are given by the zeros of $W(\sigma)$. By repeating the calculation of W for different values of σ, we obtain W as a function of σ. The zeros of W are then obtained by interpolation and by successive approximation, as in Newton's methods giving both the σ_1 and the corresponding eigenfunctions, $\zeta_1(y)$.